Age ranges of the Tibetan ice cores with emphasis on the Chongce ice cores,

western Kunlun Mountains

Shugui Hou[1,2], Theo M. Jenk[3,4], Wangbin Zhang[1], Chaomin Wang[1], Shuangye Wu[5],

5   Yetang Wang[6], Hongxi Pang[1] and Margit Schwikowski[3, 4]

[1]School of Geographic and Oceanographic Sciences, Nanjing University, Nanjing,

210023, China.

[2]CAS Center for Excellence in Tibetan Plateau Earth Sciences, Beijing, 100101,

10   China.

[3]Laboratory of Environmental Chemistry, Paul Scherrer Institute, CH-5232 Villigen

PSI, Switzerland.

[4]Oeschger Centre for Climate Change Research, University of Bern, Sidlerstrasse 5,

CH-3012 Bern, Switzerland.

15   [5]Department of Geology, University of Dayton, Dayton, OH 45469, USA.

[6]College of Geography and Environment, Shandong Normal University, Jinan,

250358, China.

Correspondence to: Shugui Hou (shugui@nju.edu.cn)

Abstract. An accurate chronology is the essential first step for a sound understanding

20 of ice core records, however, dating of ice cores drilled from the high elevation

glaciers is challenging and often problematic, leading to great uncertainties. The

Guliya ice core, drilled to bedrock (308.6 m in length) from the western Kunlun

Mountains on the northwestern Tibetan Plateau (TP) and widely used as a benchmark

for paleoclimate research, is believed to reach > 500 ka (thousand years) at its bottom.

25 Meanwhile other Tibetan ice cores (i.e., Dasuopu and East Rongbuk in the Himalayas,

Puruogangri in the central TP, and Dunde in the northeastern TP) are mostly of the

Holocene origin. In this study, we drilled four ice cores to bedrock (216.6 m, 208.6 m,

135.8 m and 133.8 m in length, respectively) from the Chongce ice cap ~30 km from

the Guliya ice core drilling site. We performed measurements of ^{14}C, ^{210}Pb, tritium

30 and β-activity for the ice cores, and used these values in a two-parameter flow

model to establish the ice core depth-age relationship. We suggested that the Chongce

ice cores might be of Holocene origin, consistent to the other Tibetan ice cores except

Guliya. The remarkable discrepancy between the Guliya and all the other Tibetan ice

core chronology implies that more effort is necessary to explore multiple dating

35   techniques to confirm the age ranges of the TP glaciers, including those from

Chongce and Guliya.

1 Introduction

Ice cores from the Tibetan Plateau (TP) provide a wealth of information for past

40   climatic and environmental conditions that extends beyond the instrumental period

(e.g., Thompson et al., 1989; 1997; 2000). An accurate chronology is the essential

first step for a sound understanding of such ice core records. However, ice core dating

is always a challenging task because seasonal signals suitable for annual layer

counting are usually only observable in top sections of ice cores. For deeper (older)

45   sections, annual cycles cannot be identified due to rapid thinning of ice layers. If

sufficient organic matter (e.g., plant or insect fragments) is found inside the ice cores,

the conventional radiocarbon (^{14}C) dating can be used (Thompson et al., 2002). If

Unfortunately, the presence of such material is far from guaranteed, which limits its

application for ice core dating. Recently, a novel method was developed to extract

50   water-insoluble organic carbon (WIOC) particles at microgram level from

carbonaceous aerosol embedded in the glacier ice for Accelerator Mass Spectrometry

(AMS) ^{14}C dating (Jenk et al., 2007; Uglietti et al., 2016). Carbonaceous aerosol is

constantly transported to the glaciers, where it is deposited and finally incorporated in

glacier ice. Consequently, carbonaceous aerosol in ice cores can provide reliable

55   dating at any given depth when the samples contain sufficient carbon mass (> 10 μ

g). Here we applied this recently established technique for dating the Tibetan ice

cores.

2 Chronology of previous ice cores

60   There are quite a few ice cores to the bedrock ever drilled from TP (Fig. 1). Below we

review briefly information available about the bottom ages of these ice cores. Please

refer to their original literatures for more details.

The Dunde ice cores: In 1987, three ice cores to bedrock (139.8 m, 136.6 m and 138.4

m in length) were recovered at an altitude of 5325 m a.s.l from the Dunde ice cap (38°

65   06′ N, 96° 24′ E) in the Qilian Shan on the northern TP (Fig. 1). Surface and basal

borehole temperatures were -7.3 °C and -4.7 °C, respectively. The 2 ‰ shift in $\delta^{18}O$,

concurrent with a sudden increase in dust concentration 14 m above the bedrock was

interpreted as evidence of glacial-stage ice (Thompson et al., 1989). The core was

extrapolated to 40 ka B.P. at the depth of 5 m above the bedrock by applying a two

70   dimensional flow model, and was suggested to be potentially more than 100 ka B.P. at

the ice-bedrock contact (Thompson et al., 1989). Later, Thompson et al. (2005)

provided a single ^{14}C date of 6.24±0.33 ka B.P. for a sample collected close to the

ice–bedrock contact (exact distance above the contact unavailable), and suggested the

possibility that this core may be of Holocene origin.

75   The Guliya ice core: In 1992, a 308.6 m ice core to bedrock was recovered at an

elevation of 6200 m a.s.l. from the Guliya ice cap (35° 17′ N, 81° 29′ E) in the

western Kunlun Mountains on the northwestern TP (Fig. 1). The Guliya ice cap is

surrounded by vertical ice walls 30 to 40 m high and has internal temperatures of

-15.6 °C at 10 m, -5.9 °C at 200 m, and -2.1 °C at its base. Top 266 m of the Guliya

80   core was dated to a period spanning 110 ka B.P., and the ice below 290 m was

suggested to be >500 ka B.P., or to ~760 ka B.P. at the ice-bedrock contact based on

[36]Cl-dead ice at the bottom section (Thompson et al., 1997).

The Dasuopu ice cores: In 1997, three ice cores were drilled from the Dasuopu glacier

(28° 23′ N, 85° 43′ E) in the Himalayas. The first core (159.9 m in length) was

85   drilled at an altitude of 7000 m a.s.l., and two more cores (149.2 and 167.7 m in

length, respectively) were drilled to bedrock 100 m apart on the col at an altitude of

7200 m a.s.l. (Thompson et al., 2000). Borehole temperatures were -16 °C at 10 m

and −13 °C at the ice/bedrock contact (Yao et al., 2002). The $\delta^{18}O$ record of the

Dasuopu ice core lacks the 5 to 6 ‰ depletion that characterises glacial stage ice from

90   the tropics to the polar regions (Yao et al., 2002). Furthermore, Dasuopu's basal ice

does not contain as low as 0.4 ppmv (parts per million by volume) methane levels that

characterise glacial ice in polar ice cores (Raynaud et al., 2000). Thus, it was

suggested that the Dasuopu ice field accumulated entirely during the Holocene

(Thompson et al., 2005).

95   The Puruogangri ice cores: In 2000, three ice cores (118.4 m, 214.7 m and 152 m in

length) were recovered at an altitude of 6070 m a.s.l. from the Puruogangri ice cap (33°

55′ N, 89° 05′ E) on the central TP (Fig. 1). Borehole temperatures were −9.7 °C at

10 m and −5 °C at the ice/bedrock contact. The measured oldest ^{14}C date is 6.44±0.16

ka B.P. at 210.5 m depth of the 214.7 m ice core. The dating was extrapolated another

100   0.5 m further down to 7 ka B.P. (Thompson et al., 2006). The Puruogangri ice cores

were suggested to be of Holocene origin (Thompson et al., 2005).

The East Rongbuk ice cores: In 2001, one ice core to bedrock (117.1 m in length) was

drilled on the col of East Rongbuk Glacier (28° 1′ N, 86° 58′ E, 6518 m a.s.l.) on the

north slope of Qomolangma (Mount Everest) in the Himalayas. In 2002, two more ice

105   cores (108.8 m and 95.8 m in length, respectively) were drilled to bedrock nearby the

previously drilling site. In a previous study, we matched the CH_4/ $\delta^{18}O_{atm}$ phase

record of both the East Rongbuk 117.1 m and 108.8 m cores to the GRIP CH_4 and the

GISP2 $\delta^{18}O_{atm}$ of the Greenland summit ice cores, and the results suggest a

Holocene origin of the East Rongbuk ice cores (Hou et al., 2004).

110   The Grigoriev ice core: In 2007, an ice core to bedrock (86.87 m long) was recovered

at an altitude of 4563 m a.s.l at the top of the Grigoriev ice cap (41° 59′ N, 77° 55′

E) in the west Tien Shan (Fig. 1). Borehole temperatures were was -2.7 °C at 10 m

and −3.9 °C at the ice/bedrock contact. Takeuchi et al. (2014) suggested that the

bottom age of the Grigoriev ice core coincides with the Younger Dryas cold period

115 (YD, 11.7 - 12.9 ka B.P.). However, the oldest ^{14}C age (12.58±0.10 ka) is obtained

from a soil sample collected underneath the glacier, which should be considered as an

upper constraint for the age of ice at the ice-bedrock contact.

3 The Chongce ice cores

120 In 2012, we drilled two ice cores to bedrock with length of 133.8 m (Core 1) and

135.8 m (Core 2) and a shallow core (Core 3) of 58.8 m at an altitude of 6010 m a.s.l.

from the Chongce ice cap on the northwestern TP (35º14′ N, 81º7′ E; Fig. 1). The

direct distance between the Chongce and the Guliya ice core drilling sites is ~30 km

(Fig. S1). In 2013, two more ice cores were recovered to bedrock with the length of

125 216.6 m (Core 4) and 208.6 m (Core 5) at an altitude of 6100 m a.s.l. on the Chongce

ice cap (35°15′ N, 81°5′ E). The detailed positions of the five Chongce ice

cores are shown in Fig. S2. Borehole temperatures are -12.8 °C, -12.6 °C and -12.6 °C

at 10 m depth for Core 1, Core 2 and Core 3, -8.8 °C and -8.8 °C at 130 m depth for

Core 1 and Core 2, respectively (Fig. S3), suggesting that the Chongce ice cap is

130 frozen to its bedrock. The Density profiles of the Chongce Core 2, Core 3 and Core 4

are shown in Fig. S4. All the ice cores were transported frozen to the cold room in the

Nanjing University for further processing. The basal sediment collected from the

bottom of Core 4 was measured for the first luminescence dating, resulting in an age

of 42±4 ka B.P., which was regarded as an upper constraint for the age of the bottom

135   ice at the drilling site (Zhang et al., 2018).

4 Measurements

^{14}C

140   We performed ^{14}C measurements on WIOC extracted from 22 samples collected

discretely along the 216.6 m Chongce Core 4 and 9 samples along the 135.8 m

Chongce Core 2, as well as 5 samples collected from the East Rongbuk 95.8 m ice

core. The ^{14}C sample decontamination was performed at Paul Scherrer Institute by

removing the ~3 mm outer layer with a bandsaw in a -20 °C cold room and rinsing

145   with ultra-pure water in a class 100 laminar flow box. The WIOC fraction of

carbonaceous particles in the sample was filtered onto freshly preheated quartz fiber

filters (Pallflex Tissuquartz, 2500QAO-UP), then combusted stepwise (10 min at

340 °C; 12 min at 650 °C) using a thermal-optical carbon analyzer (Model4L, Sunset

Laboratory Inc., USA) for separating organic carbon (OC) from elemental carbon

150   (EC), and the resulting CO_2 was measured by the Mini Carbon Dating System

(MICADAS) with a gas ion source for ^{14}C analysis at the University of Bern LARA

laboratory. Details about sample preparation procedures and analytical methods can

be found in previous studies (Jenk et al., 2007, 2009; Sigl et al., 2009; Uglietti et al.,

2016). The overall procedural blanks were estimated using artificial ice blocks of

155   frozen ultra-pure water, which were treated the same way as real ice samples. The

average overall procedural blank is 1.34±0.62　μg carbon with a $F^{14}C$ of 0.69±0.13

(Uglietti et al., 2016). Conventional ^{14}C ages were calibrated using OxCal v4.2.4

software with the IntCal13 calibration curve (Bronk Ramsey and Lee, 2013; Reimer

et al., 2013).

160

[210]Pb

The accessible time range using radioactive isotope ^{210}Pb dating is ~150 years due to

the 22.3-year half-life of ^{210}Pb, a product of the natural ^{238}U decay series. Here ^{210}Pb

dating was performed on the Chongce 216.6 m Core 4, with a total of 52 samples

165 collected from the depth of 0-76.6 m. Each sample (~100 - 200 g) was cut parallel to

the drilling axis in a -20 °C cold room. The samples were processed according to the

standard method established by Gäggeler et al. (1983). The samples were melted for

24 hours after adding 0.05% (V:V) analytical reagent HCl (30%). Afterwards, 100 μ

L ^{209}Po tracer was added to the solution to determine the yield of the separation.

170 Spontaneous deposition of Po on an Ag disk (15 mm diameter), which was fixed on a

wire and immersed in the liquid, was achieved during ~7 hours at 95 °C in 500 mL

Erlenmeyer flasks using a magnetic stirrer. After drying, the disks were measured by

α -counting at the Paul Scherrer Institute. The samples were positioned in vacuum

chambers at a distance of 1mm from silicon surface barrier detectors (ORTEC,

175 ruggedized, 300 and 450 mm^2) having an α -energy resolution of ~23 keV full width

at half-maximum at 5.3 MeV. The yield of ^{209}Po tracer was measured via its 4.9 MeV

α -line. Typical chemical yields were ~75%.

Tritium

180   Tritium measurements were performed on the Chongce 216.6 m Core 4, with 51

samples collected successively from the depth range of 6.7-11.8 m (corresponding to

a sampling resolution of ~ 0.1 m per sample), and 42 samples from the depth range of

11.8-32.0 m (corresponding to a sampling resolution of ~ 0.5 m per sample). Each

sample is ~10 g. Samples were analyzed at the Paul Scherrer Institute using liquid

185   scintillation counting (TriCarb 2770 SLL/BGO, Packard SA). The detection limit for

3H measurements is <10 TU.

β-activity

Twenty-two samples were collected successively from top to the depth of 10.3 m of

190   the Chongce 58.8 m Core 3. Each sample is ~1 kg. The β-activity was measured

using Alpha-Beta Multidetector (Mini 20, Eurisys Mesures) at the National Key

Laboratory of Cryospheric Sciences, China. More details can be found in An et al.

(2016).

195 5 Results

The β-activity profile of the Chongce 58.8 m Core 3 is shown in Fig. 2a. A β

-activity peak at the depth of 8.2-8.4 m was referenced as 1963 AD, while a second

β-activity peak at the depth of 4.8-5.1 m was set as 1986 AD, corresponding to the

1986 Chernobyl nuclear accident. Both β-activity peaks were also observed in the

200   Muztagata ice core from the eastern Pamir (Tian et al., 2007). The calculated mean

annual accumulation rate is 140 mm w.e. (water equivalent) /year for the period of

1963–2012 AD.

The tritium profile of the Chongce 216.6 m Core 4 is shown in Fig. 2b. The tritium

activity was corrected for decay to the time of deposition, because our purpose is to

205   identify the apparent tritium peak (3237±89 TU) at the depth of 21.4 m. The depth of

the sample with the highest activity was related to the year 1963, the year that the

atmospheric test ban treaty was signed and tritium levels in precipitation began to

decline gradually because of radioactive decay and the cessation of atmospheric

testing (e.g. Kendall and Doctor, 2003). The calculated mean annual accumulation

210   rate is 297 mm w.e./year for the period of 1963-2013 AD.

The ^{210}Pb activity profile of the Chongce 216.6 m Core 4 is shown in Fig. 3, which

shows an exponential decrease as a function of depth in line with the radioactive

decay law. The ^{210}Pb activity concentrations are in the range 7.5-317 mBq/kg, but

keep relatively stable for the lower 16 samples, with an average of 11.2±2.1 mBq/kg

215   (not shown). This average was taken as background ^{210}Pb (BGD) from the mineral

dust contained in the ice core and was subtracted from the measured ^{210}Pb activity

concentrations. From the linear regression of the logarithmic ^{210}Pb activities (BGD

subtracted) against depth (Fig. 3), the value of the axis intercept (236±33 mBq/kg)

corresponds to the ^{210}Pb activity at the surface of the Chongce ice cap. Following the

220   widely applied approach described by Gäggeler et al. (1983), the ice age was derived

using the constant initial concentration (CIC) model of equation (1). We calculated

1891±15 AD at the depth of 44.09 m (i.e. 34.36 m w.e.), resulting in a mean annual

net accumulation rate of 280±47 mm w.e./year for the period of 1891-2013 AD. This

value is in very good agreement with the 297 mm w.e./year for the period of

225   1963-2013 AD derived from the tritium profile of the same ice core (i.e., the Chongce

216.6 m Core 4, Fig. 2b).

$$t_s = \lambda^{-1} ln\left(\frac{C_0}{C_S}\right) \qquad\qquad (1)$$

Where, t_s stands for the age of ice at a certain depth with ^{210}Pb activities (subtracted)

C_S, λ for the decay constant of [210]Pb (0.03114 a^{-1}), and C_0 for the ^{210}Pb surface

230 activity.

The ^{14}C age profiles of the Chongce 216.6 m Core 4 and the 135.8 m Core 2 are

shown in Figs 4 and 5, and the results are given in Tables S1 and S2, respectively. We

initially collected the ^{14}C samples taking into consideration of the chronology of the

Guliya ice core, but finally realized that most of the samples, especially those

235 collected from the upper sections, are too young to be dated with an acceptable

uncertainty. For instance, we obtained 1891±15 AD at the depth of 44.09 m from the

[210]Pb measurements (Fig. 3), and the ^{14}C ages are 0.013-0.269 ka cal B.P. at the depth

of 40.11-40.97 m, and modern to 0.430 ka cal B.P. at 50.06-50.82 m. Even though all

obtained calibrated age ranges of the uppermost four samples include the expected

240 ages based on the ^{210}Pb dating results, they have large uncertainties due to the young

age and the relatively flat shape of the calibration curve in the past 500 yrs.

Furthermore, anthropogenic contribution for samples younger than 200 yrs is likely

introduce an old bias in ^{14}C ages due to fossil fuel (^{14}C dead) contribution (Jenk et al.,

2006). Only 2% fossil contribution would shift the mean of the calibrated age ranges

245   for these samples by up to 200 yrs towards younger ages, resulting in a smaller age

range close to the ages estimated by ^{210}Pb dating. The ^{14}C age profile in the depth

range of 80-180 m shows large scatter and no clear increase in age (Fig. 4). This is

likely caused by the relatively young age of samples in combination with relatively

large analytical uncertainties due to the presence of high mineral dust load in the

250   Chongce ice core.

We made use of the ^{14}C ages (excluding the top four samples for the reasons

discussed above), the ^{210}Pb results (Fig. 3), and the tritium horizon (Fig. 2) to

establish the depth-age relationship for the Chongce 216.6 m Core 4 (Fig. 4), by

applying a two-parameter flow model (2p model) (Bolzan, 1985 and Supplement). To

255   avoid overfitting of the data and giving to much weight to individual data points, we

prefer not to make assumptions about changes in accumulation, such as by applying a

Monte-Carlo approach (Uglietti et al., 2016; Gabrielli et al., 2016). However, we

understand that the 2p model, though widely used for establishing the ice core

chronology including the Dunde (Thompson et al., 1989) and the Puruogangri

260 (Thompson et al., 2006) ice cores, is limited and cannot account for the complex flow

regimes close to the glacier bedrock. Therefore, we simply used the flow model to fit

the dating points for obtaining a continuous age-depth scale. In order to make full use

of the information available, we estimated the age at the ice-bedrock by extrapolating

2p model to the bedrock. The results of the bottom ages were provided in Supplement.

265

6 Discussion

We have notice the apparent incoherence between the depth-age relationship of Core

2 and Core 4, which may be caused by their surface topography, resulting in different

accumulation rate at their respective drilling sites. The mean annual accumulation rate

270 of Core 3 (several meters away from Core 2 drilling site) is calculated to be 140 mm

w.e. /year for the period of 1963–2012 AD, while the mean annual accumulation rate

of Core 4 is 297 mm w.e./year for the period of 1963-2013 AD. It is possible that the

Core 4 drilling site may receive extra snow supplies, such as snow drifting, whereas

part of the snow deposition at the Core 3 drilling site may be blown away due to wind

275   scouring (Fisher et al., 1983). The impact of wind scouring on the ice core drilled

from the Dasuopu summit was also suggested (Thompson et al., 2018). Nevertheless,

a full understanding of this difference will require a long-term *in situ* observation that

is unavailable at this moment.

It was previously suggested that the Himalayan ice cores (Dasuopu and East Rongbuk)

280   were of Holocene origin (Thompson et al., 2005; Hou et al., 2004). The oldest cal. ^{14}C

age for a sample collected down to the ice-bedrock contact of the East Rongbuk 95.8

m ice core, is 6.72±0.43 ka B.P., confirming its Holocene origin. The ice cores from

Puruogangri in the central TP, and, to a less degree, Dunde in the northeastern TP are

of Holocene origin, too (Thompson et al., 2005). For the Chongce ice cores, the

285   measured oldest cal. ^{14}C ages are similar to what are measured for the East Rongbuk,

Puruogangri and Dunde ice cores (Fig. 1). Our estimated ages at the ice-bedrock

contact ($8.3\pm_{3.6}^{6.2}$ ka B.P. for the Chongce 216.6 m Core 4 and $9.0\pm_{3.6}^{7.9}$ ka B.P. for the

Chongce 135.8 m Core 2 respectively, see details in Supplement) are either of

Holocene origin, or, less possible, origin of late deglaciation period, similar to the

290   result of the Grigoriev ice core in the west Tien Shan (Takeuchi et al., 2014). In both

cases, the results confirm the upper constraint of 42±4 ka B.P. derived from the

luminescence age of the basal sediment sample collected from the bottom of the

Chongce 216.6 m Core 4 (Zhang et al., 2018).

It is apparent that the age range of the Guliya ice core is, at least, an order of

295   magnitude older than that of the other Tibetan and the Tien Shan ice cores. Thompson

et al. (2005) previously considered this as evidence that the growth (glaciation) and

decay (deglaciation) of large ice fields in the lower latitudes are often asynchronous.

However, our new understanding of the chronology of the Chongce ice cores suggests

a similar age range of the ice cores in the western Kunlun Mountains in comparison to

300   the other Tibetan cores. Though the validity of the Guliya chronology has been

assumed since its publication (Thompson et al., 2005, 2017), Cheng et al. (2012)

argued that the Guliya ice core chronology should be shortened by a factor of two in

order to reconcile the difference in the $\delta^{18}O$ variations between the Guliya ice core

and the Kesang stalagmite records (Fig. 1 and Supplement). Although, at this

305   moment, we cannot give the final word on the age ranges of the Tibetan ice cores, it is

necessary to explore more indepentant evidences to decipher the age dilemma of the

ice cores from the western Kunlun Mountains on the northwestern TP.

We notice that, in 2015, a new Guliya ice core to bedrock (309.73 m in length) was

drilled close to the location of the 1992 Guliya core drill site. Thompson et al. (2018)

310   suggested that future analyses will include ^{14}C, ^{36}Cl, ^{10}Be, δ^{18}O of air in bubbles,

and argon isotopic ratios (^{40}Ar/^{38}Ar) on deep sections of the new Guliya ice core to

determine more precisely the age of the Guliya ice cap. We look forward to their new

results.

315   **7 Conclusions**

We provided cal. ^{14}C ages and age estimation at the ice-bedrock contact of the

Chongce ice cores drilled from the western Kunlun Mountains on the northwestern

Tibetan Plateau, where exceptional length of the ice core record was previously

suggested. Our results suggest that the age ranges of the Chongce ice cores is similar

320   to the other Tibetan ice cores except the Guliya ice core, confirming the recent

conclusion derived from the luminescence age of the Chongce ice core. The current

work may has wide implications, such as whether or not existance of asynchronous

glaciation on the Tibetan Plateau. Undoubtly, more effort is necessary to explore

multiple dating techniques to confirm the ages of the Tibetan glaciers, including those

325   from Chongce and Guliya.

References

An, W., Hou, S., Zhang, W., Wu, S., Xu, H., Pang, H., Wang, Y., and Liu, Y.:

Possible recent warming hiatus on the northwestern Tibetan Plateau derived

345   from ice core records, Sci. Rep., 6, 32813, doi:10.1038/srep32813, 2016.

Bolzan, J.: Ice flow at the Dome C ice divide based on a deep temperature profile, J.

Geophys. Res., 90, 8111-8124, 1985.

Bronk Ramsey, C. and Lee, S.: Recent and planned developments of the program

Oxcal, Radiocarbon, 55, 720-730, doi:10.2458/azu_js_rc.55.16215, 2013.

350   Cheng, H., Zhang, P. Z., Spötl, C., Edwards, R. L., Cai, Y. J., Zhang, D. Z., Sang, W.

C., Tan, M., and An, Z. S.: The climatic cyclicity in semiarid-arid central Asia

over the past 500,000 years, Geophys. Res. Lett., 39, L01705,

doi:10.1029/2011GL050202, 2012.

Fisher, D., Koerner, R., Paterson, W., Dansgaard, W., Gundestrup, N., and Reeh, N.:

355   Effect of wind scouring on climatic records from ice-core oxygen-isotope

profiles, Nature, 301, 205-209, doi: 10.1038/301205a0, 1983.

Gabrielli, P. et al.: Age of the Mt. Ortles ice cores, the Tyrolean Iceman and glaciation

of the highest summit of South Tyrol since the Northern Hemisphere Climatic

Optimum, The Cryosphere, 10, 2779–2797, doi:10.5194/tc-10-2779-2016,

360   2016.

Gäggeler, H., von Gunten, H., Rössler, E., Oeschger, H., andSchotterer, U.:

^{210}Pb-dating of cold Alpine firn/ice cores from Colle Gnifetti, Switzerland, J.

Glaciol., 29, 165-177, 1983.

Hou, S., Qin, D., Jouzel, J., Masson-Delmotte, V., von Grafenstein, U., Landais, A.,

365   Caillon, N., and Chappellaz. J.: Age of Himalayan bottom ice cores, J. Glaciol.

50, 467-468, 2004.

Jenk, T., Szidat, S., Schwikowski, M., Gäggeler, H., Brütsch, S., Wacker, L., Synal,

H., and Saurer, M.: Radiocarbon analysis in an Alpine ice core: record of

anthropogenic and biogenic contributions to carbonaceous aerosols in the past

370   (1650–1940), Atmos. Chem. Phys., 6, 5381–5390,

doi:10.5194/acp-6-5381-2006, 2006.

Jenk, T., Szidat, S., Schwikowski, M., Gäggeler, H., Wacker, L., Synal, H., and

Saurer, M.: Microgram level radiocarbon (^{14}C) determination on carbonaceous

particles in ice, Nucl. Instrum. Methods Phys. Res. Sect. B, 259, 518-525,

375   doi:10.1016/j.nimb.2007.01.196, 2007.

Jenk, T., Szidat, S., Bolius, D., Sigl, M., Gäggeler, H., Wacker, L., Ruff, M.,

Barbante, C., Boutron, C., and Schwikowski, M.: A novel radiocarbon dating

technique applied to an ice core from the Alps indicating late Pleistocen ages,

J. Geophys. Res., 114, D14, doi:10.1029/2009jd011860, 2009.

380   Kendall, C. and Doctor, D. H.: Stable isotope applications in hydrologic studies,

Treatise on Geochemistry, 5, 319-364, doi:10.1016/B0-08-043751-6/05081-7,

2003.

Raynaud, D., Barnola, J., Chappellaz, J., Blunier, T., Indermühle, A., and Stauffer, B.:

The ice core record of greenhouse gases: a view in the context of future

385   changes, Quat. Sci. Rev., 19, 9–17, 2000.

Reimer, P., Bard, E., Bayliss, A., Beck, J., Blackwell, P., Ramsey, C., Buck, C.,

Cheng, H., Edwards, P., Friedrich, M., Grootes, P., Guilderson, T., Haflidason,

H., Hajdas, I., Hatté, C., Heaton, T., Hoffmann, D., Hogg, A., Hughen, K.,

Kaiser, K., Kromer, B., Manning, S., Niu, M., Reimer, R., Richards, D., Scott,

390   E., Southon, J., Staff, R., Turney, C., and van der Plicht, J.: IntCal13 and

Marine13 radiocarbon age calibration curves 0-50,000 years cal B.P.,

Radiocarbon, 55, 1869-1887, doi:10.2458/azu_js_rc.55.16947, 2013.

Sigl, M., Jenk, T., Kellerhals, T., Szidat, S., Gäggeler, H., Wacker, L., Synal, H.,

Boutron, C., Barbante, C., Gabrieli, J., and Schwikowski, M.: Towards

395   radiocarbon dating of ice cores, J. Glaciol., 55, 985-996,

doi:10.3189/002214309790794922, 2009.

Takeuchi, N., Fujita, K., Aizen, V., Narama, C., Yokoyama, Y., Okamoto, S., Naoki,

K., and Kubota, J.: The disappearance of glaciers in the Tien Shan Mountains

in Central Asia at the end of Pleistocene, Quat. Sci. Rev., 103, 26-33,

400   doi:10.1016/j.quascirev.2014.09.006, 2014.

Thompson, L. G., Mosley-Thompson, E., Davis, M., Bolzan, J., Dai, J., Klein, L.,

Yao, T., Wu, X., Xie, Z., and Gundestrup, N.: Holocene-late pleistocene

climatic ice core records from Qinghai-Tibetan Plateau, Science, 246,

474-477, doi:10.1126/science.246.4929.474, 1989.

405   Thompson, L. G., Yao, T., Davis, M. E., Henderson, K. A., Mosley-Thompson, E.,

Lin, P.-N., Beer, J., Synal, H.-A., Cole-Dai, J., and Bolzan, J.F.: Tropical

climate instability: the last glacial cycle from a Qinghai-Tibetan ice core,

Science, 276, 1821-1825, doi: 10.1126/science.276.5320.1821, 1997.

Thompson, L. G., Yao, T., Mosley-Thompson, E., Davis, M., Henderson, K., and Lin,

410   P.: A high-resolution millennial record of the south Asian monsoon from

Himalayan ice cores, Science, 289, 1916-1919, 2000.

Thompson, L. G., Mosley-Thompson, E., Davis, M., Henderson, Brecher, H.,

Zagorodnov, V., Mashiotta, T., Lin, P., Mikhalenko, V., Hardy, D., and Beer,

J.: Kilimanjaro ice core records: evidence of Holocene climate change in

415   tropical Africa, Science, 298, 589-593, 2002.

Thompson, L. G., Davis, M., Mosley-Thompson, E., Lin, P., Henderson, K., and

Mashiotta, T.: Tropical ice core records: evidence for asynchronous glaciation

on Milankovitch timescales, J. Quat. Sci., 20, 723-733, 2005.

Thompson, L. G., Yao, T., Davis, M., Mosley-Thompson, E., Mashiotta, T., Lin, P.,

420   Mikhalenko, V., and Zagorodnov, V.: Holocene climate variability archived in

the Puruogangri ice cap on the central Tibetan Plateau, Ann. Glaciol., 43,

61-69, 2006.

Thompson, L.: Past, present, and future of glacier archives from the world's highest

mountains, Proc. Am. Philos. Soc., 161, 226-243, 2017.

425 Thompson, L., Yao, T., Davis, M., Mosley-Thompson, E., Wu, G., Porter, S., Xu, B.,

Lin, P.,   Wang, N., Beaudon, E., Duan, K., Sierra-Hernández, M., and Kenny,

D.: Ice core records of climate variability on the Third Pole with emphasis on

the Guliya ice cap, western Kunlun Mountains, Quat. Sci. Rev., 188, 1-14,

doi:10.1016/j.quascirev.2018.03.003, 2018.

430   Tian, L., Yao, T., Wu, G., Li, Z., Xu, B., and Li, Y.: Chernobyl nuclear accident

revealed from the 7010 m Muztagata ice core record, Chin. Sci. Bull., 52,

1436-1439, doi: 10.1007/s11434-007-0188-y, 2007.

Uglietti, C., Zapf, A., Jenk, T., Sigl, M., Szidat, S., Salazar, G., and Schwikowski, M.:

Radiocarbon dating of glacier ice: overview, optimisation, validation and

435   potential, The Cryosphere 10, 3091-3105, doi:10.5194/tc-10-3091-2016, 2016.

Yao, T., Duan, K., Xu, B., Wang, N., and Pu, J.: Temperature and methane changes

over the past 1000 years recorded in Dasuopu glacier (central Himalaya) ice

core, Ann. Glaciol., 35, 379–383, 2002.

Yao, T., Masson-Delmotte, V., Gao, J., Yu, W., Yang, X., Risi, C., Sturm, C., Werner,

440   M., Zhao, H., He, Y., Ren, W., Tian, L., Shi, C., and Hou, S.: A review of

climatic controls on $\delta^{18}O$ in precipitation over the Tibetan Plateau:

Observations and simulations, Rev. Geophys., 51, 525–548,

doi:10.1002/rog.20023, 2013.

Zhang, Z., Hou, S., and Yi, S.: The first luminescence dating of Tibetan glacier basal

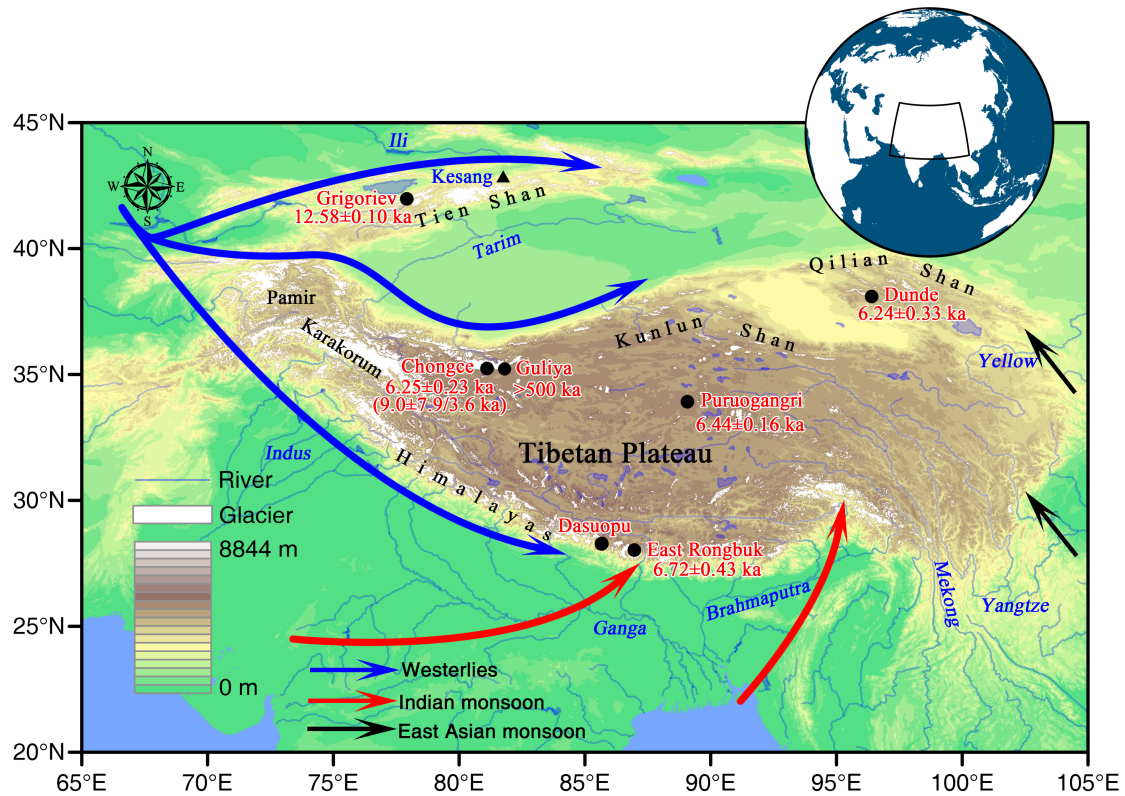445   sediment, The Cryosphere, 12, 1-6, doi:10.5194/tc-12-1-2018, 2018.

Figure 1: Map showing the locations of ice core drilling sites. The numbers for each

site except Guliya are the measured oldest ^{14}C ages, while the number inside the

bracket below the Chongce site is the estimated ice age at the ice-bedrock contact.

The schematic positions of the westerlies and the monsoon circulations are from Yao

et al. (2013). Data of glaciers are from the Global Land Ice Measurements from Space

(GLIMS, available at http://www.glims.org). The topographic data were extracted

using ETOPO1 elevations global data, available from National Oceanic and

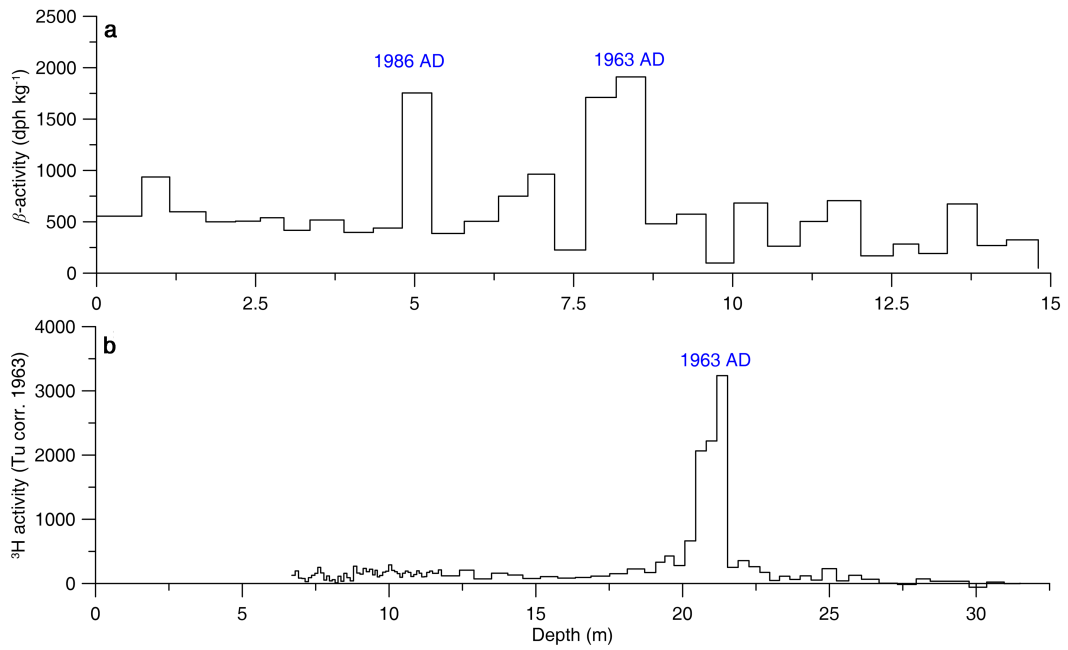Atmospheric Administration at http://www.ngdc.noaa.gov/mgg/global/global.html.

Figure 2: The *β*-activity profile of the Chongce 58.8 m Core 3 (a) and the tritium

460   (corrected for the decay) profile of the Chongce 216.6 m Core 4 (b). TU (tritium units)
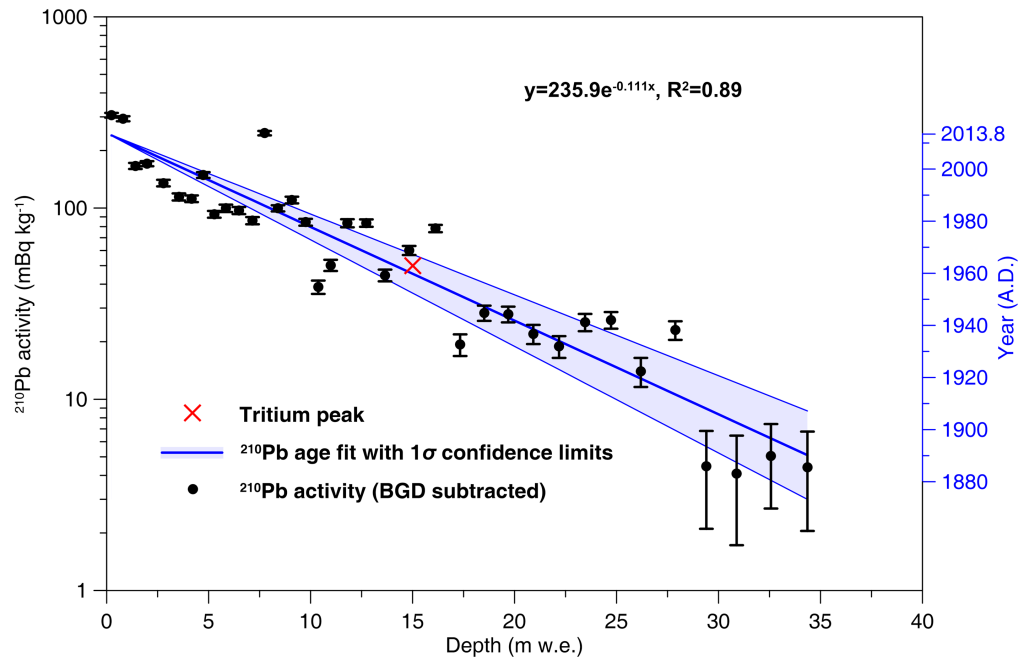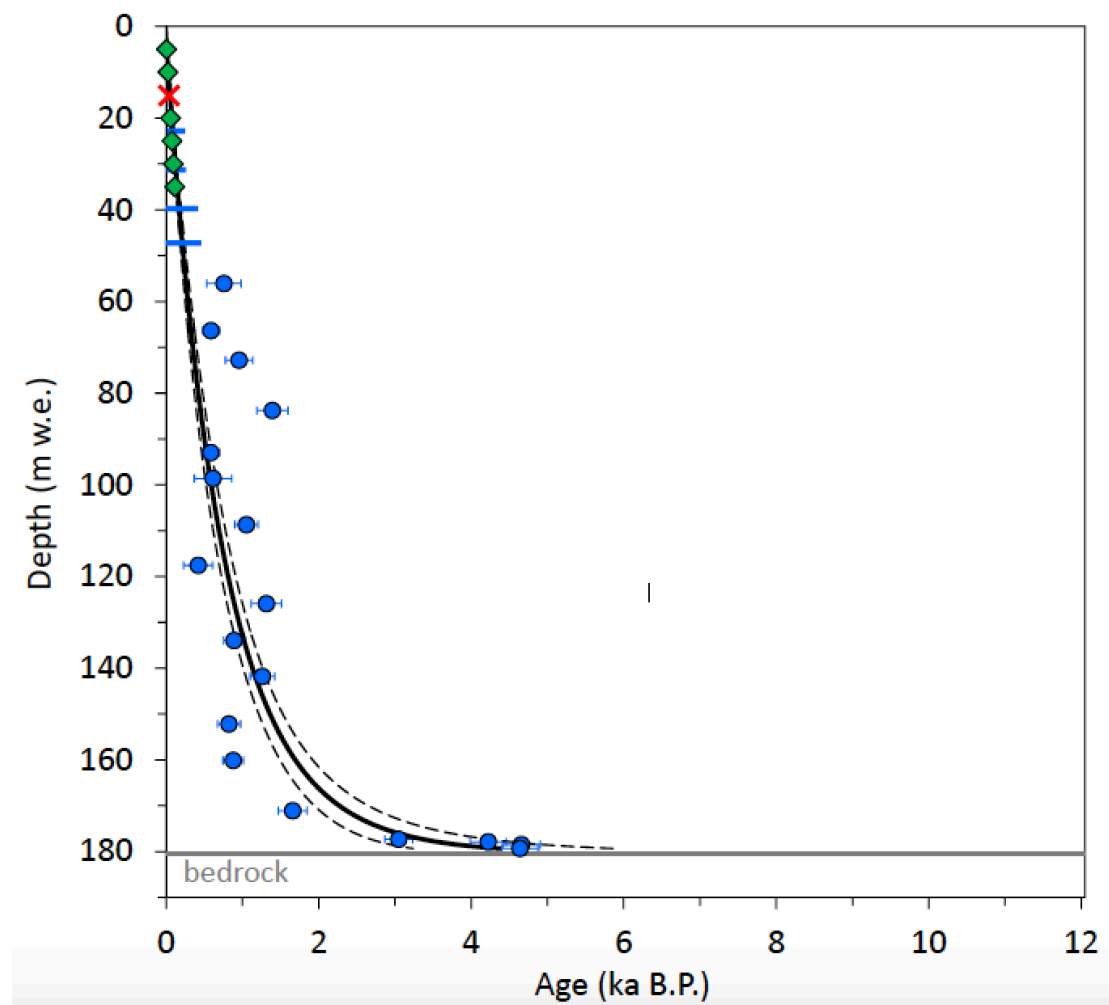
is one tritium atom/1018 hydrogen atoms.

Figure 3: ^{210}Pb activity profile of the Chongce 216.6 m Core 4 and the derived

465   age-depth relationship. The ^{3}H fallout horizon indicating the year 1963 A.D. is

located within the uncertainty of the ^{210}Pb results. Please note that the 1 σ confidence

band is related to the right hand y-axis only.

470 Figure 4: The depth-age relationship of the Chongce 216.6 m Core 4. The dashed

lines represent the 1 σ confidence interval of the 2p model fit (solid line). The red

cross stands for the tritium horizon, green diamonds for the ^{210}Pb ages calculated at

intervals of 5 m w.e. (Fig. 3), and the blue dots for the cal. ^{14}C ages with 1 σ error
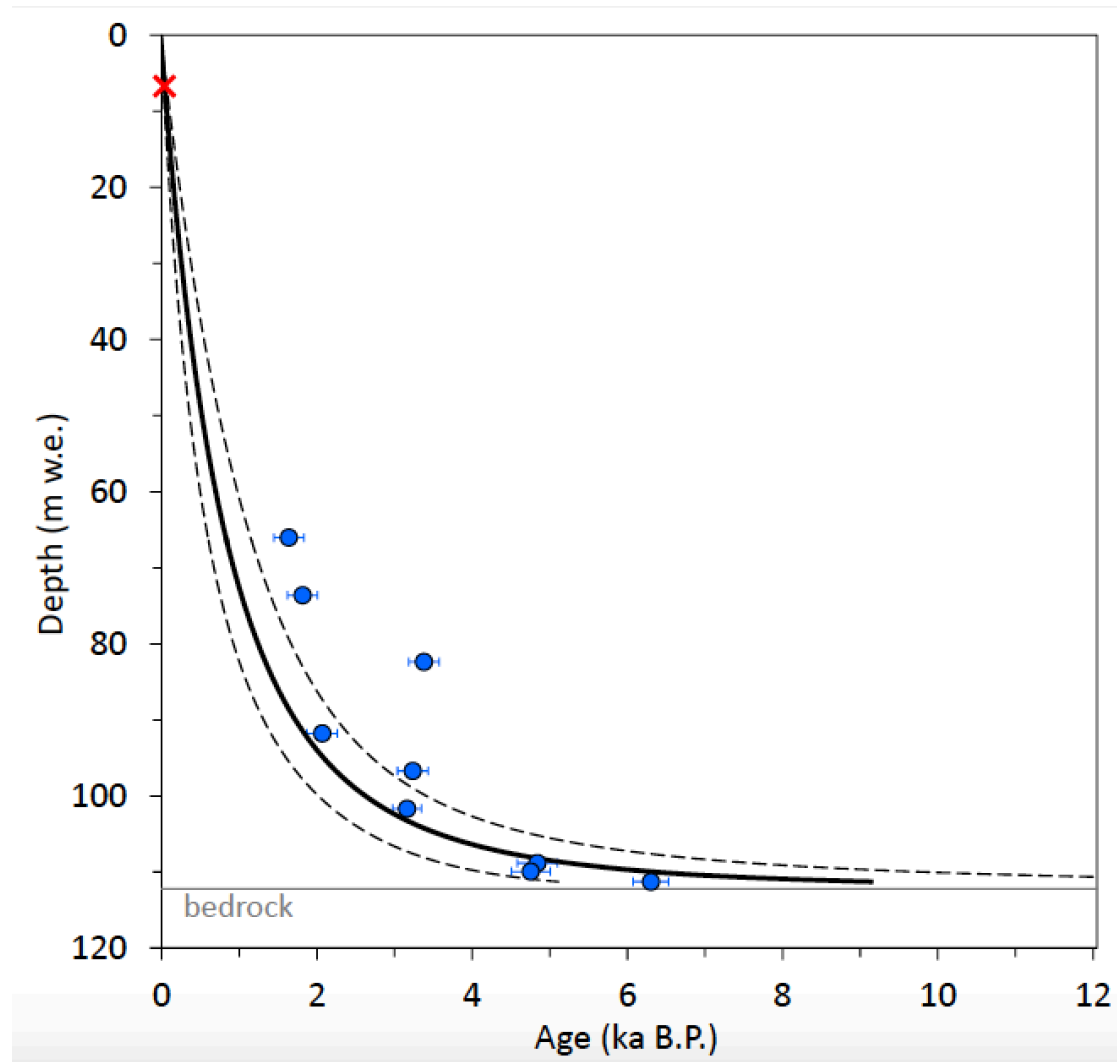
bar.

475

Figure 5: The depth-age relationship of the Chongce 135.8 m Core 2. The dashed

lines represent the 1σ confidence interval of the 2p model fit (solid line). The red

cross stands for the β-activity horizon (Fig. 2) and the blue dots for the cal. ^{14}C ages

with 1 σ error bars.